

# Preorganized Ligand Arrays Based on Spirotetrahydrofuryl Motifs. Synthesis of the Stereoisomeric 1,8,14-Trioxatrispiro[4.1.4.1.4.1]octadecanes and the Contrasting Conformational Features and Ionic Binding Capacities of These Belted Ionophores

Leo A. Paquette,\* Jinsung Tae, Eugene R. Hickey, William E. Trego, and Robin D. Rogers<sup>†</sup>

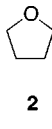
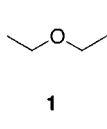
Evans Chemical Laboratories, The Ohio State University, Columbus, Ohio 43210, and Department of Chemistry, The University of Alabama, Tuscaloosa, Alabama 35487

paquette.1@osu.edu

Received October 2, 2000

The cis,trans trispiro ether **4** is accessible from several synthetic directions as a consequence of a crossover in reaction selectivity when proceeding from nucleophilic attack on the cis dispiro ketone to oxygenation of the  $\alpha,\beta$ -unsaturated ester **17**. Its cis,cis isomer **3** was obtained in 17 steps and 14.6% overall yield from 3,5-dimethoxybenzoic acid by making use of the alicyclic side chain in **N** as a “conformational lock”. Although **4** shows no measurable tendency to complex with alkali metal ions, **3** binds strongly to  $\text{Li}^+$  and  $\text{Na}^+$  ions, as well as to  $\text{CH}_3\text{NH}_3^+$ . Whereas the **3eq** conformation is populated in the solid state and in solution, complex formation occurs readily.  $^{13}\text{C}$  NMR studies have defined slow exchange limits as the 2:1 sandwich complex with lithium ion is initially formed and transformed progressively into a 1:1 species upon the addition of more  $\text{LiClO}_4$ . Only the 2:1 complex with sodium ion is formed during comparable titration with  $\text{NaClO}_4$ . Association constants, molecular mechanics calculations, and X-ray crystallographic studies provide insight into the binding capacity of this belted tridentate ionophore.

The differing physical properties of diethyl ether (**1**) and its cyclic dehydro congener tetrahydrofuran (**2**), while extraordinary, are often taken for granted. For example,



advantage is routinely taken of the complete miscibility of THF with water and the contrasting limited aqueous solubility of ether. It is also widely recognized that the progression from an acyclic to a cyclic ether significantly affects intrinsic basicity, with THF exhibiting greater hydrogen bonding capability,<sup>1</sup> enhanced gas-phase proton affinity,<sup>2</sup> and faster rate of proton attachment in solution.<sup>3</sup> Many of the natural ionophores utilize cyclic ether fragments as ligand arrays for ionic recognition and transport.<sup>4</sup> In the latter context, the inherent stereochemistry of these arrays make matters particularly

conducive to the population of those conformations well suited to metal ion binding.<sup>5</sup> The incorporation of oxygen-containing rings in favorable topological arrangements is of continuing importance in the synthesis of preorganized receptors of chemical and biological relevance.<sup>6–12</sup>

(4) (a) Gokel, G. *Crown Ethers and Cryptands*; The Royal Society of Chemistry: Cambridge, England, 1991. (b) Cooper, S. R., Ed. *Crown Compounds: Toward Future Applications*; VCH Publishers: New York, 1992. (c) Vögtle, F. *Supramolecular Chemistry*; John Wiley and Sons: Chichester, England, 1991. (d) Inoue, Y.; Gokel, G. W. *Cation Binding by Macrocycles*; Marcel Dekker: New York, 1990. (e) Westley, W. J., Ed. *Polyether Antibiotics*; Marcel Dekker: New York, 1983; Vols. I and II. (f) Dobler, M. *Ionophores and Their Structures*; Wiley-Interscience: New York, 1981. (g) Izatt, R. M.; Christensen, J. J. *Synthetic Multidentate Macroyclic Compounds*; Academic Press: New York, 1978.

(5) (a) Kilburn, J. D.; Patel, H. K. *Contemp. Org. Synth.* **1994**, *1*, 259. (b) Izatt, R. M.; Pawlak, K.; Bradshaw, J. S.; Bruening, R. L. *Chem. Rev.* **1991**, *91*, 1721. (c) Schneider, H.-J. *Angew. Chem., Int. Ed. Engl.* **1991**, *30*, 1417. (d) Cram, D. J. *Angew. Chem., Int. Ed. Engl.* **1988**, *27*, 1009.

(6) (a) Li, G.; Still, W. C. *J. Am. Chem. Soc.* **1993**, *115*, 3804. (b) Wang, X.; Erickson, S. D.; Iimori, T.; Still, W. C. *J. Am. Chem. Soc.* **1992**, *114*, 4128. (c) Li, G.; Still, W. C. *J. Org. Chem.* **1991**, *56*, 6964. (d) Erickson, S. D.; Still, W. C. *Tetrahedron Lett.* **1990**, *31*, 4253. (e) Iimori, T.; Still, W. C.; Rheingold, A. L.; Staley, D. L. *J. Am. Chem. Soc.* **1989**, *111*, 3439.

(7) (a) Burke, S. D.; McDermott, T. S.; O'Donnell, C. J. *J. Org. Chem.* **1998**, *63*, 2715. (b) Burke, S. D.; Heap, C. R.; Porter, W. J.; Song, Y. *Tetrahedron Lett.* **1996**, *37*, 343. (c) Burke, S. D.; O'Donnell, C. J.; Porter, W. J.; Song, Y. *J. Am. Chem. Soc.* **1995**, *117*, 12649.

(8) (a) McGarvey, G. J.; Stepanian, M. W.; Bressette, A. R.; Ellena, J. F. *Tetrahedron Lett.* **1996**, *37*, 5465. (b) McGarvey, G. J.; Stepanian, M. W. *Tetrahedron Lett.* **1996**, *37*, 5461.

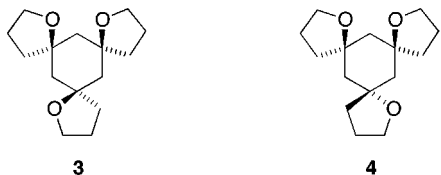
(9) (a) Koert, U.; Stein, M.; Wagner, H. *Liebigs Ann.* **1995**, 1415. (b) Koert, U.; Stein, M.; Harms, K. *Angew. Chem., Int. Ed. Engl.* **1994**, *33*, 1180.

(10) Mehta, G.; Vidya, R. *Tetrahedron Lett.* **1997**, *38*, 4173, 4177.

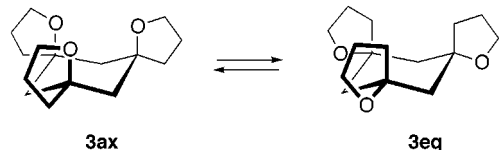
(11) (a) Lee, W. Y.; Park, C. H. *J. Org. Chem.* **1993**, *58*, 7149. (b) Lee, W. Y.; Park, C. H.; Kim, S. J. *Am. Chem. Soc.* **1993**, *115*, 1184.

(12) (a) Hormuth, S.; Schade, W.; Reissig, H.-U. *Liebigs Ann.* **1996**, 2001.

In view of the central position held by substituted tetrahydrofurans in natural ionophores and their enhanced capacity for chelation, we have sought to exploit this binding efficacy by designing and synthesizing belted spirocyclic polyether networks.<sup>13</sup> With level of substitution, locus of the oxygen atoms, and relative stereochemistry as relevant principles of rational design, it was anticipated that heightened levels of structural preorganization could be achieved. This paper focuses on the trispiro cyclohexanes **3** and **4**. The *cis,cis* isomer **3** clearly

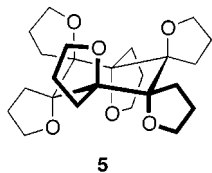


enjoys a level of binding-site convergence and complementarity not available to **4**. As a consequence, the cumulative noncovalent interactions capable of materializing in **3** when its three C–O bonds are axially disposed were expected to qualify this isomer, but not **4**, as an effective host molecule for the smaller alkali metal ions. The cyclohexane belt confers a defined spatial relationship among the tetrahydrofuran subunits while not instilling absolute rigidity. Thus, the spirocyclic nature of the substituent rings was expected to facilitate rather than inhibit the interconversion of **3ax** with **3eq**.<sup>14</sup> As



will be seen, the preferential adoption of one or the other of these conformers is less predictable, since the conformational bias is controlled by a complex interplay of steric and electronic effects.<sup>15</sup> However, these incremental preferences should be overridden by favorable ligation, at least as far as lithium and sodium ions are concerned.

Finally, we point out that while **3** is capable of coordination uniquely in a monofacial sense, it represents the logical starting point for the development of a class of *bifacial*/ligands typified by **5**.<sup>16a</sup> Such structurally defined compounds are of interest because they feature extended



(13) (a) Negri, J. T.; Rogers, R. D.; Paquette, L. A. *J. Am. Chem. Soc.* **1991**, *113*, 5073. (b) Paquette, L. A.; Negri, J. T.; Rogers, R. D. *J. Org. Chem.* **1992**, *57*, 3947. (c) Paquette, L. A.; Stepanian, M.; Mallavadhani, U. V.; Cutarelli, T. D.; Lowinger, T. B.; Klemeyer, H. *J. J. Org. Chem.* **1996**, *61*, 7492.

(14) The requirement that three ether oxygens or three methylene groups must be syn-axially oriented will result in appreciable flattening of the cyclohexane chair. Further, the 1,3,5-placement of the spiro rings does not introduce vicinal eclipsing during ring inversion. Both of these factors are expected to contribute to a lowering of the barrier associated with conformational flexing in both the forward and reverse directions. For a discussion of associated issues, consult: Eliel, E. L.; Wilen, S. H.; Mander, L. N. *Stereochemistry of Carbon Compounds*; John Wiley and Sons: New York, 1994; pp 686–720.

three-dimensional features not previously examined in the context of crown ethers and offer scenarios having potential application in many areas of investigation.

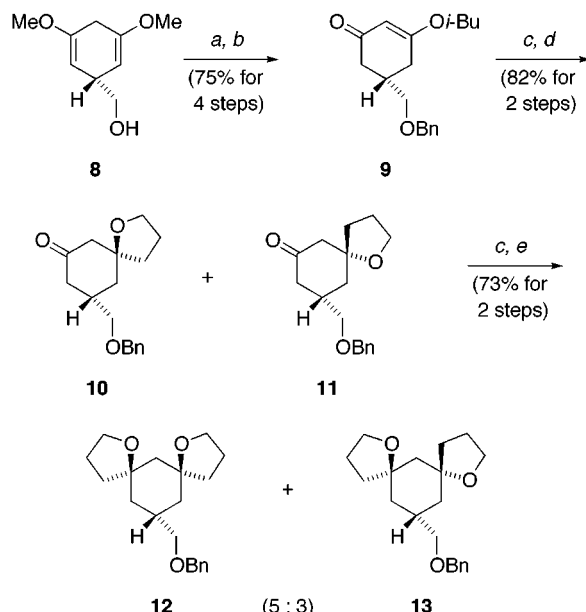
## Synthetic Considerations

**Routes That Lead to the Trans Isomer.** In an earlier paper,<sup>16b</sup> we reported that potential access routes to **3** and **4** by way of the *meso*- and *dl*-diols **6** and **7**,



respectively, are plagued with high inefficiency at several steps. The neopentyl nature of the carbinol centers was one of the contributory causes. The present synthetic strategy skirts this problem by involving 3,5-dimethoxybenzoic acid as the triply functionalized precursor. The sequential Birch reduction and lithium aluminum hydride treatment of this inexpensive benzenoid compound to give **8** has been detailed previously.<sup>17</sup> Subsequent *O*-benzylation of alcohol **8** in advance of exposure to isobutyl alcohol in the presence of a catalytic quantity of concentrated sulfuric acid produced **9**<sup>18</sup> (Scheme 1). This

**Scheme 1<sup>a</sup>**



<sup>a</sup> Key: (a) NaH, BnBr; (b) *i*-BuOH, conc H<sub>2</sub>SO<sub>4</sub>; (c) ClMg(CH<sub>2</sub>)<sub>3</sub>O-MgCl; 1 N HCl; (d) TsOH, CH<sub>2</sub>Cl<sub>2</sub>; (e) TsCl, Et<sub>3</sub>N.

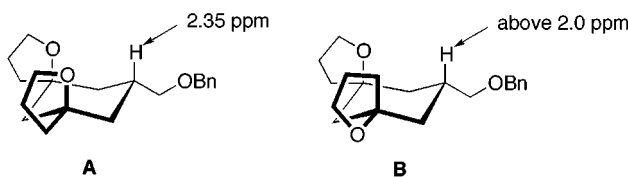
5-substituted 3-alkoxycyclohexenone afforded, following coupling to the Normant reagent<sup>19</sup> and hydrolysis with

(15) (a) Paquette, L. A.; Branan, B. M.; Stepanian, M. *Tetrahedron Lett.* **1996**, *37*, 1721. (b) Paquette, L. A.; Stepanian, M.; Branan, B. M.; Edmondson, S. D.; Bauer, C. B.; Rogers, R. D. *J. Am. Chem. Soc.* **1996**, *118*, 4505. (c) Paquette, L. A.; Bolin, D. G.; Stepanian, M.; Branan, B. M.; Mallavadhani, U. V.; Tae, J.; Eisenberg, S. W. E.; Rogers, R. D. *J. Am. Chem. Soc.* **1998**, *120*, 11603.

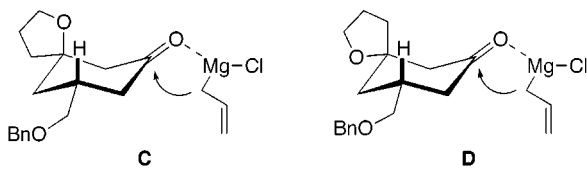
(16) (a) Paquette, L. A.; Tae, J.; Branen, B. M.; Eisenberg, S. W. E.; Hofferberth, J. E. *Angew Chem. Int. Ed.* **1999**, *38*, 1412. (b) Paquette, L. A.; Stearns, B. A.; Mooney, P. A.; Tae, J. *Heterocycles* **1999**, *50*, 27. (c) For a preliminary communication of the present results, consult Paquette, L. A.; Tae, J.; Hickey, E. R.; Rogers, R. D. *Angew. Chem., Int. Ed. Engl.* **1999**, *38*, 1409.

(17) (a) Wilkie, J. S.; Winzenberg, K. N. *Austr. J. Chem.* **1989**, 42, 1207. (b) Nishikawa, T.; Isobe, M. *Tetrahedron* **1994**, 50, 5621.

1 N HCl, an approximate 1:1 mixture of the enone and cyclized monospiro ketones. Complete conversion to **10** and **11** was easily accomplished with *p*-toluenesulfonic acid in CH<sub>2</sub>Cl<sub>2</sub>. Although **10** and **11** proved not to be easily purified due to difficulties with  $\beta$ -elimination, their more advanced capping with additional Normant reagent gave rise to a chromatographically separable 5:3 mixture of **12** and **13**. These isomers are readily distinguished both structurally and conformationally. Thus, the *C*<sub>2</sub> symmetry of **12** is evident on the basis of its 13-line <sup>13</sup>C NMR spectrum (**13** is characterized by 18 peaks). Beyond that, the cis isomer (*R*<sub>f</sub> = 0.2 in 1:1 hexanes/ethyl acetate) is appreciably more polar than its trans counterpart (*R*<sub>f</sub> = 0.7), and exhibits an axial methine proton that is highly deshielded (compare **A** and **B**). These data confirm that the two oxygens in **12** are oriented axially at ambient temperature.



In complementary studies, the mixture of spiro ketones **10** and **11** was coupled to both allylmagnesium bromide and the allylindium reagent. As expected,<sup>20</sup> the ether oxygens are too remote from the electrophilic carbon center to affect the stereochemistry of the reaction. In fact, both organometallic reagents gave rise to the same 5:3 mixture of **14** and **15** (Scheme 2). Following their chromatographic separation, these carbinols were individually cyclized in a two-step sequence featuring hydroboration to again provide **12** and **13**. In light of these observations, it is apparent that the two diastereomeric monospiro ketones are attacked preferably from the equatorial direction as reflected in **C** and **D**, and to the same degree.



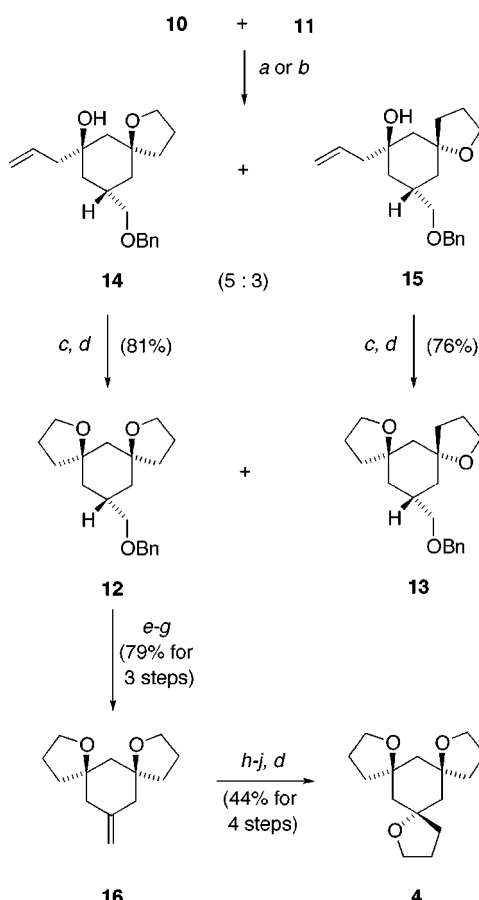
The stage was now set to proceed with an elimination in **12**. Following hydrogenolytic cleavage of the benzyl group, dehydration was indirectly, but smoothly, implemented via the *o*-nitrophenyl selenocyanate.<sup>21</sup> The resulting exomethylene derivative **16** was subsequently ozonolyzed to provide the labile cis spiro cyclohexanone which was treated immediately with allylmagnesium bromide in THF at 0 °C. Under these conditions, no evidence was uncovered for the generation of  $\beta$ -elimination products. In contrast, the Normant reagent channeled matters completely in this undesirable direction. Capping of the single carbinol isolated from the Grignard

(18) The free alcohol derived from **9** has been previously described: (a) Reference 17b. (b) Grieco, P. A.; Dai, Y. *J. Am. Chem. Soc.* **1998**, *120*, 5128.

(19) Cahiez, G.; Alexakis, A.; Normant, J. F. *Tetrahedron Lett.* **1978**, *3013*.

(20) Paquette, L. A.; Lobben, P. C. *J. Org. Chem.* **1998**, *63*, 5604.

(21) Grieco, P. S.; Gilman, S.; Nishizawa, M. *J. Org. Chem.* **1976**, *41*, 1485.

Scheme 2<sup>a</sup>

<sup>a</sup> Key: (a) BrMgCH<sub>2</sub>CH=CH<sub>2</sub>, THF (83%); (b) BrCH<sub>2</sub>CH=CH<sub>2</sub>, In, THF (83%); (c) BH<sub>3</sub>·THF; H<sub>2</sub>O<sub>2</sub>, NaOH; (d) TsCl, Et<sub>3</sub>N; (e) H<sub>2</sub>, 10% Pd/C, EtOH, 40 psi; (f) *o*-(NO<sub>2</sub>)PhSeCN, Bu<sub>3</sub>P, THF; (g) 30% H<sub>2</sub>O<sub>2</sub>, THF; (h) O<sub>3</sub>, MeOH/CH<sub>2</sub>Cl<sub>2</sub>; Me<sub>3</sub>S; (i) BrMgCH<sub>2</sub>CH=CH<sub>2</sub>; (j) BH<sub>3</sub>; NaOOH.

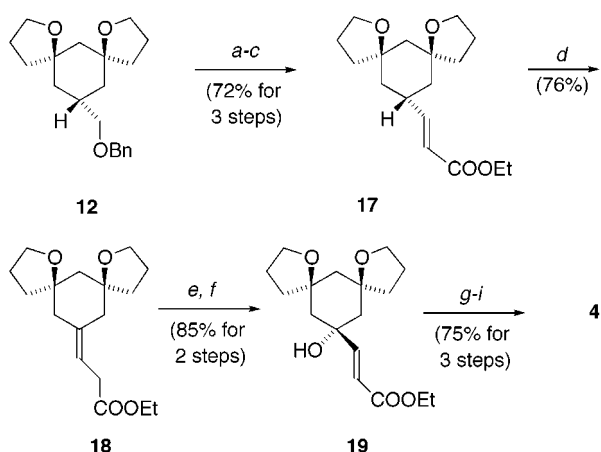
reaction led unmistakably to the *C*<sub>2</sub>-symmetric **4**. This trispiro ether exhibits a 10-line <sup>13</sup>C NMR spectrum and average polarity. Discussion of the conformational ramifications associated with the stereochemical course of this allylmagnesium bromide addition is deferred to a later segment of this paper.

The second synthetic thrust relied on a deconjugation-epoxidation sequence.<sup>22</sup> The cis spiro aldehyde **20** was homologated under Wadsworth-Emmons conditions,<sup>23</sup> giving **17** in 72% overall yield from **12** (Scheme 3). When this ester was treated with potassium hexamethyldisilazide in THF-HMPA at -78 °C, little chemical change was noted. Warming of such reaction mixtures to 0 °C resulted in rapid decomposition. Fortunately, deconjugation was seen to proceed well at -15 °C without destruction of the reactant, affording **18** in 76% isolated yield. Epoxidation of **18** with *m*-chloroperbenzoic acid<sup>24</sup> and subsequent  $\beta$ -elimination in the presence of DBU afforded **19** as the only stereoisomeric product. The relative stereochemistry of this carbinol was established by a sequence of steps involving hydrogenation, lithium aluminum hydride reduction, and cyclization of the

(22) Ikeda, Y.; Ukai, J.; Ikeda, N.; Yamamoto, H. *Tetrahedron* **1987**, *43*, 743.

(23) Wadsworth, W. S. *J. Org. React.* **1977**, *25*, 73.

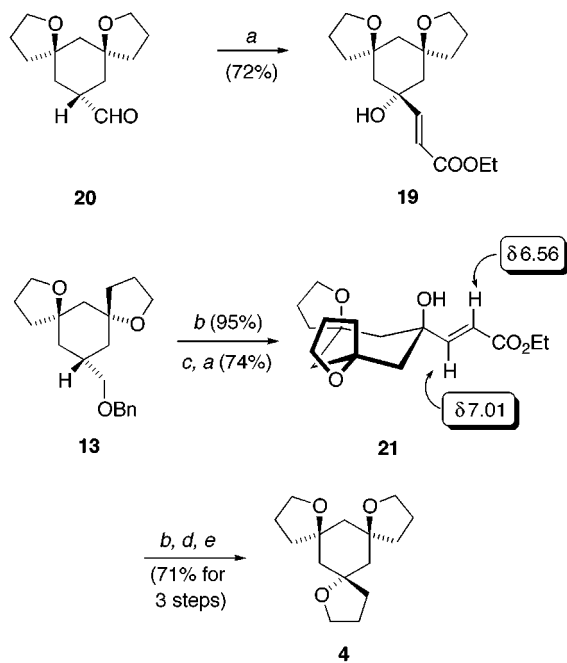
(24) Attempted oxidation of **18** with dimethyldioxirane resulted in exclusive attack of the activated methylene group  $\alpha$  to the carbethoxy group.

Scheme 3<sup>a</sup>

<sup>a</sup> Key: (a)  $H_2$ , 10% Pd/C, EtOH, 40 psi; (b) Swern,  $CH_2Cl_2$ ; (c)  $(EtO)_2P(=O)OCH_2COOEt$ , DBU, LiCl,  $CH_3CN$ ; (d) KHMDS, THF/HMPA,  $-78 \rightarrow -15^\circ C$ ; satd  $NH_4Cl$ ,  $-78^\circ C$ ; (e) *m*-CPBA; (f) DBU; (g)  $H_2$ , 10% Pd/C; (h) LiAlH<sub>4</sub>; (i) TsCl, Et<sub>3</sub>N.

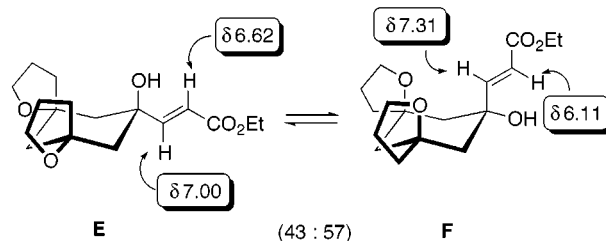
monotosylate. The resulting colorless oil was identical in all respects to the sample of **4** generated earlier. Consequently, there must occur a clean stereochemical crossover during peracid attack on the double bond in **18** relative to allylation of the corresponding ketone under Grignard conditions.

To gain a broader perspective on this stereoselectivity issue, **20** was condensed with 4-chlorophenylsulfinyl acetate in the presence of piperidine.<sup>25-28</sup> The ensuing SPAC reaction<sup>27</sup> proceeds by consecutive Knoevenagel condensation, C=C double bond shift, [2,3]-sigmatropic rearrangement, and hydrolysis to deliver the  $\gamma$ -hydroxy- $\alpha,\beta$ -unsaturated ester directly. Application of this simple procedure to **20** gave rise exclusively to **19** (Scheme 4). As before, this substance shows one spot on TLC, but is conformationally dynamic on the <sup>1</sup>H and <sup>13</sup>C NMR time scales at room temperature. Integration of several sets

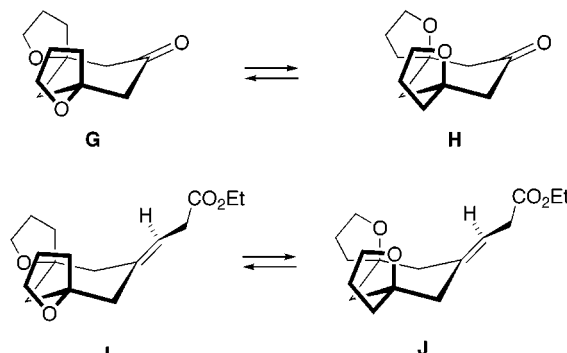
Scheme 4<sup>a</sup>

<sup>a</sup> Key: (a) *p*-(Cl)PhS(=O)CH<sub>2</sub>COOEt, piperidine,  $CH_3CN$ , reflux; (b)  $H_2/10\%$  Pd/C; (c) Swern; (d) LiAlH<sub>4</sub>; (e) TsCl, Et<sub>3</sub>N.

of signals showed the conformer having its hydroxyl group projected equatorially as in **F** to be dominant (57%). This assignment was made possible by spectral comparison with **21** prepared independently from the trans dispiro aldehyde. Especially noteworthy is the very appreciable downfield shift of  $H_\beta$  ( $\delta$  7.31) in major conformer **F**. This deshielding necessarily arises as a consequence of proximity to both axial oxygens as shown. In contrast, the two vinylic protons in minor conformational isomer **E** ( $H_\alpha$ ,  $\delta$  6.62;  $H_\beta$ ,  $\delta$  7.00) are closely similar to those of the conformationally stable **21** ( $H_\alpha$ ,  $\delta$  6.56;  $H_\beta$ ,  $\delta$  7.01). While the favored status accorded to **F** has interesting implications, the  $K_{eq}$  is too small to warrant extensive discussion.



**Conformational Characteristics of Functionalized Cis Dispiro Cyclohexanes.** The cis dispirocyclohexane prepared in this investigation and its homologated  $\alpha,\beta$ -unsaturated ester **17** share in common the capacity for equilibrating between two chair conformers<sup>13b,29</sup> as **G** ⇌ **H** and **I** ⇌ **J**, respectively. The consequence of



these ring inversions is the exchange of two equatorially disposed C–O bonds with two axial C–C bonds and vice-versa. Since neither substance is crystalline and their <sup>1</sup>H NMR spectra exhibit an appreciable overlapping of signals, direct experimental analysis of the preferred conformation in each instance has not been possible. However, when the two structures were subjected to a standard Monte Carlo conformational search by way of the MacroModel software package (version 5.0)<sup>30</sup> and the

(25) (a) Yamagawa, S.; Sato, H.; Hoshi, N.; Kosugi, H.; Uda, H. *J. Chem. Soc., Perkin Trans. 1* **1979**, 570. (b) Nokami, J.; Mandai, T.; Imakura, Y.; Nishiuchi, K.; Kawada, M.; Wakabayashi, S. *Tetrahedron Lett.* **1981**, 22, 4489.

(26) (a) Tanikaga, R.; Nozaki, Y.; Tanakaga, K.; Kaji, A. *Chem. Lett.* **1982**, 1703. (b) Tanikaga, R.; Nozaki, Y.; Tamura, T.; Kaji, A. *Synthesis* **1983**, 134.

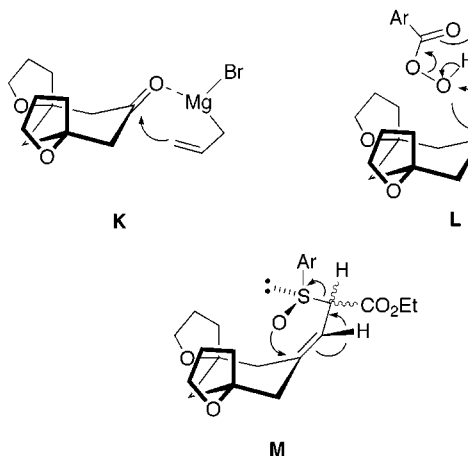
(27) Corey, E. J.; Carpino, P. *Tetrahedron Lett.* **1990**, 31, 7555.

(28) (a) Burgess, K.; Henderson, I. *Tetrahedron Lett.* **1989**, 30, 3633. (b) Burgess, K.; Cassidy, J.; Henderson, I. *J. Org. Chem.* **1991**, 56, 2050.

(29) Paquette, L. A.; Branan, B. M.; Friedrich, D.; Edmondson, S. D.; Rogers, R. D. *J. Am. Chem. Soc.* **1994**, 116, 506.

MM3-minimized results<sup>31</sup> were further refined using the full matrix Newton Raphson protocol, the energy differences were found to be quite small. The relative energies generated for gas-phase structures by this procedure favored **H** over **G** by 1.13 kcal/mol, and **I** over **J** by only 0.54 kcal/mol. These data lead us to conclude that the flattened nature of the cyclohexane "belt" in these structures diminishes the level of potential conformational dominance to vanishingly small levels. In addition, the barriers to interconversion are expected to be low as previously indicated for multispiro systems of this type.<sup>14</sup>

Notwithstanding the above, both substrates have been found to undergo highly stereoselective reactions, thereby implicating the involvement of a specific conformer during product formation. For example, Grignard addition to the ketone can be expected to proceed from the equatorial direction as foreshadowed, *inter alia*, by **C** and **D**, and with heightened levels of steric approach control. We therefore conclude, in light of the fact that **4** is ultimately formed, that the transition state must resemble **K**. Note that the two ethereal C–O bonds are equatorially disposed.<sup>32</sup>



The normal stereochemical preference of peracid epoxidation for axial attack on methylenecyclohexenes, originally discussed in terms of product development control,<sup>32a</sup> has more recently been attributed to a combination of bond torsion and rotor effects,<sup>33</sup> with possible lesser contributions from  $\sigma \rightarrow \sigma^*$  (Cieplak-type) interactions.<sup>34</sup> In the specific case of **17**, equatorial orientation of the tetrahydrofuryl oxygens can be expected to facilitate delivery of the oxygen atom as shown in **L**. This enhanced preference to involve conformer **I** is likewise encountered during the [2,3]-sigmatropic rearrangement of the sulfoxide **M**.

The magnitudes of transition state steric and torsional energy contributions to  $\Delta\Delta G^\ddagger$  are such as to pose an interesting dilemma. Since nucleophilic additions to the

(30) Mohamadi, F.; Richards, N. G. J.; Guida, W. C.; Liskamp, R.; Lipton, M.; Caufield, C.; Chang, G.; Hendrickson, T.; Still, W. C. *J. Comput. Chem.* **1990**, *11*, 440.

(31) Allinger, N. L.; Yuh, Y. H.; Lii, J.-H. *J. Am. Chem. Soc.* **1989**, *111*, 8551.

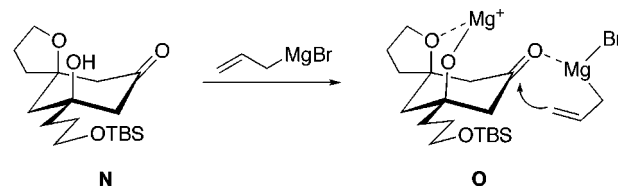
(32) (a) Carlson, R. G.; Behn, N. S. *J. Org. Chem.* **1967**, *32*, 1363. (b) Corey, E. J.; Feiner, N. F. *J. Org. Chem.* **1980**, *45*, 765.

(33) (a) Vedejs, E.; Dent, W. H., III; Kendall, J. T.; Oliver, P. A. *J. Am. Chem. Soc.* **1996**, *118*, 3556. (b) Shi, Z.; Boyd, R. J. *J. Am. Chem. Soc.* **1993**, *115*, 9614. (c) Wu, Y.-D.; Tucker, J. A.; Houk, K. N. *J. Am. Chem. Soc.* **1991**, *113*, 5018.

(34) Cieplak, A. S.; Tait, B. D.; Johnson, C. R. *J. Am. Chem. Soc.* **1989**, *111*, 8447.

ketone involve **G** and proceed via equatorial attack (see **K**), the stereoselectivity of this reaction class is *identical* to that involving oxygenation reactions of the  $\alpha,\beta$ -unsaturated ester which involve axial delivery to **I** as in **L** and **M**.

**Acquisition of the All-Cis Isomer.** Despite the fact that the reactive conformers **G** and **I** both feature equatorial C–O bonds, this structural characteristic is obviously not conducive to a stereocontrolled synthesis of **3**. A superior, more reliable control feature was therefore mandated. The more biased conformational structure **N** was considered to be favorably populated prior to closure of the second spirotetrahydrofuran ring. The silyl-protected (3-hydroxypropyl) substituent, originally introduced via allylation (Scheme 2), is sufficiently bulky (*i.e.*, comparable to ethyl) to warrant its equatorial occupancy in the lowest energy conformation.<sup>32b</sup> Furthermore, exposure of this intermediate to a Grignard reagent should be met with rapid deprotonation and formation of the chelate **O**. The two C–O bonds will now be oriented axially with significant shielding of the top face of the carbonyl group. As a consequence, the customary equatorial entry of the nucleophile should continue to operate and fix the triad of oxygens in an all-syn relationship.

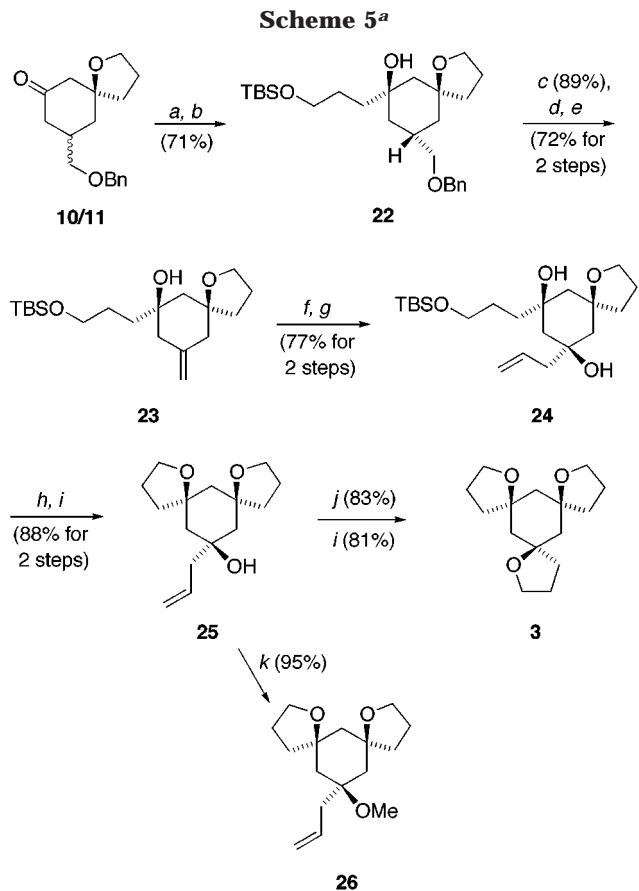


The feasibility of this strategy is demonstrated in Scheme 5. The Normant reagent was added to the **10/11** mixture as before. Following chromatographic purification, the major diol was regioselectively silylated to provide **22** in 71% yield for the two steps. Following conventional transformation of **22** into the methylenecyclohexane **23**,<sup>35</sup> the ketone was generated through ozonolysis, and coupled to allylmagnesium bromide.

Hydroboration-oxidation of the double bond in **24** was beset by problems associated with hydrolytic cleavage of the TBS substituent. The tetraol so produced is not soluble in the common organic solvents and was accordingly difficult to process. For this reason, **24** was converted into the dispiro alcohol **25** prior to activation of the allylic side chain. In this instance, the hydroxy tosylate required 15 h in refluxing  $\text{CH}_2\text{Cl}_2$  to undergo complete cyclization in the presence of DMAP. Significantly, however, only **3** was produced, as expected if the **N**  $\rightarrow$  **O** paradigm was operative. It proved an easy matter to effect the O-methylation of **25** as in **26** for comparative complexation studies to be described in the sequel.

The all-cis trispiro ether **3** is a crystalline solid, mp 111–113 °C, of  $C_{3v}$ -symmetry as revealed by the appearance of only five signals in its  $^{13}\text{C}$  NMR spectrum. The striking feature of the solid-state structure of **3** is the adoption in the crystal of the all-equatorial conformation

(35) Two minor problems were encountered during this three-step sequence. Hydrogenolysis of the benzyl ether in ethanol caused wholesale cleavage of the TBS protecting group. This unwanted reaction could be limited to the 10% level by carrying out the reduction in ethyl acetate as solvent. When the aryl selenide was oxidized with 30% hydrogen peroxide, the TBS group was again very effectively cleaved. Although reprotection could be readily accomplished, use of MCPBA as the oxidant served to bypass this complication.



<sup>a</sup> Key: (a)  $\text{ClMgO}(\text{CH}_2)_3\text{MgCl}$ , 1 N HCl; (b) TBSCl,  $\text{Et}_3\text{N}$ ; (c)  $\text{H}_2$ , 10% Pd/C,  $\text{EtOAc}$ ; (d)  $(o\text{-NO}_2)\text{PhSeCN}$ ,  $\text{Bu}_3\text{P}$ , THF; (e) m-CPBA,  $\text{CH}_2\text{Cl}_2$ ,  $-20^\circ\text{C}$ ,  $(i\text{-Pr})_2\text{NH}$ , rt; (f)  $\text{O}_3$ ,  $\text{MeOH}-\text{CH}_2\text{Cl}_2$ ,  $\text{Me}_2\text{S}$ ; (g)  $\text{BrMgCH}_2\text{CH}=\text{CH}_2$ , THF; (h) TBAF, THF; (i)  $\text{TsCl}$ ,  $\text{Et}_3\text{N}$ , DMAP,  $\text{CH}_2\text{Cl}_2$ ; (j)  $\text{BH}_3$ , THF, NaOH, 30%  $\text{H}_2\text{O}_2$ ; (k) KHMDS, THF, MeI.

**3eq** (Figure 1). These findings conflict with the gas-phase computational results realized with the MacroModel 5.0 software package. Using the energy minimization conditions described earlier, we found **3eq** to be 3.93 kcal/mol less stable than **3ax**. For comparison purposes, the two conformers generated for *cis,trans* isomer **4** by this procedure favored **P** over **Q** by a smaller margin (1.24 kcal/mol). Recourse to calculations at a higher dielectric would likely result in much smaller energy differences.

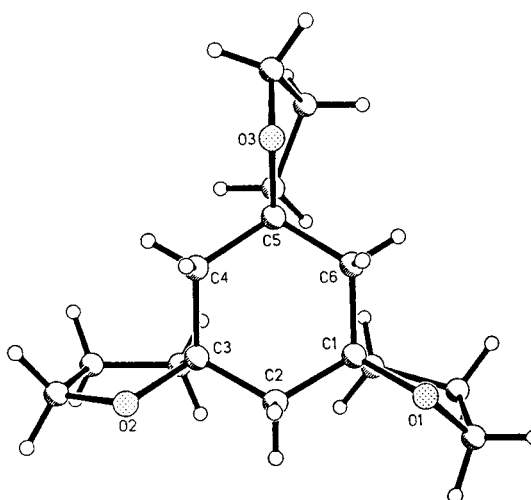
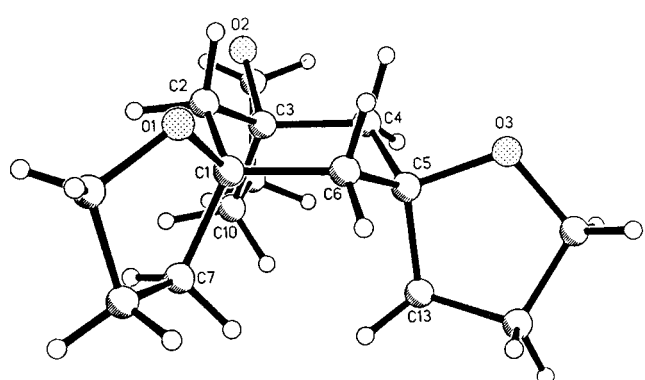


The preference for axial oxygen occupancy in the gas phase presumably arises from an interplay between the torsional requirements of the three sets of geminal C(quat)-O and C(quat)-CH<sub>2</sub> bonds. Nonbonded axial-axial CH<sub>2</sub> - - CH<sub>2</sub> repulsions probably disfavor **3eq** and **Q** despite the fact that flattening of the cyclohexane ring diminishes these steric interactions to some degree. The preference for adoption of **3eq** in the crystal lattice suggests that intermolecular stacking interactions may make a contribution to the observed packing. The dominant effect may be the avoidance of collinear, axially oriented C-O-C dipoles in **3ax**. Their intermolecular juxtapositioning could well promote the population of **3eq**.

## Complexation Studies

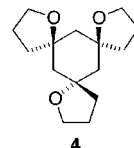
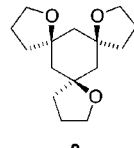
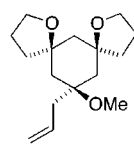
**Determination of Association Constants.** The association constants ( $K_a$ ) for **3**, **4**, and **26** were determined relative to  $\text{Li}^+$ ,  $\text{Na}^+$ , and  $\text{K}^+$  picrates in a  $\text{H}_2\text{O}-\text{CDCl}_3$  solvent mixture according to Cram's extraction method. These data, along with comparative values for 15-crown-5, are listed in Table 1. The assumption is made that the high relative concentrations of picrate salts used in these measurements normalize matters to dealing with 1:1 complexes only. From the outset, the inability of **4** to measurably extract any of the picrate salts demonstrated how dramatically a change at a single stereocenter can affect the strength and specificity with which oxophilic metal ions are bound. The all-cis trispiro ether **3** has strong chelating ability for  $\text{Li}^+$ , over 2 orders of magnitude higher than that exhibited by 15-crown-5. This ligand also exhibits a significant binding capacity for  $\text{Na}^+$  that is on a par with that shown by the simple crown ether. The  $K_a$  for  $\text{K}^+$  ( $3.3 \times 10^4$ ) is much weaker, thereby indicating that potassium ion is too large to reside comfortably in the binding pocket.

The monomethoxy derivative **26** displays only a small reduction of binding ability to  $\text{Li}^+$  relative to **3**, but a considerably lessened capacity for coordination to  $\text{Na}^+$ . This ligand exhibited a  $K_a$  for  $\text{K}^+$  ( $6.5 \times 10^3$ ), which we



**Figure 1.** Perspective plot of **3** as determined by X-ray crystallography.

**Table 1. Association Constants ( $K_a$ ) Determined by Picrate Extraction into Chloroform at 20 °C<sup>a</sup>**

$[M^+]_{aq}$	$[Pic^-]_{aq}$	$[host]_{org}$	$\xrightleftharpoons{K_a}$	$[M^+Pic^- host]_{org}$
			$Li^+$	
			$Na^+$	$K^+$
15-crown-5 <sup>b</sup>			$1.0 \times 10^5$	$4.1 \times 10^6$
			$0.94 \times 10^5$	$6.3 \times 10^6$
			$K_a(Li^+)/K_a(Na^+) = 0.015$	
			$K_a(Na^+)/K_a(K^+) = 5.7$	
			$K_a(Li^+)/K_a(K^+) = 0.085$	
			no extraction	no extraction
<b>4</b>	<b>3</b>	<b>26</b>		no extraction
			$7.9 \times 10^7$	$2.5 \times 10^6$
			$K_a(Li^+)/K_a(Na^+) = 32$	
			$K_a(Na^+)/K_a(K^+) = 76$	
			$K_a(Li^+)/K_a(K^+) = 2400$	
			$1.1 \times 10^7$	$1.3 \times 10^5$
			$K_a(Li^+)/K_a(Na^+) = 85$	$6.5 \times 10^3$

<sup>a</sup> The method developed by Koenig et al. (Koenig, K. E.; Lein, G. M.; Struckler, P.; Kaneda, T.; Cram, D. *J. Am. Chem. Soc.* **1979**, *101*, 3553) was utilized. <sup>b</sup> Values previously reported by: Erickson, S. D.; Still, W. C. *Tetrahedron Lett.* **1990**, *30*, 4235. See also: Inoue, Y.; Amano, F.; Okada, N.; Inada, H.; Ouchi, M.; Tai, A.; Kakushi, T.; Lin, Y.; Tong, L.-H. *J. Chem. Soc., Perkin Trans. 2* **1990**, 1239.

consider as too small to be significant.<sup>6e,d</sup> Increased selectivity for  $Li^+$  relative to larger  $Na^+$  and  $K^+$  ions constitutes a pattern often observed for branched crown ethers.

The consequence of belting as in **3** and **26** is, however, quite special. The observed high selectivities for  $Li^+$  apparent in these tridentate examples ( $K_a^{Li}/K_a^{Na} = 32$  and 85, respectively) is comparable to values reported for highly preorganized spherands<sup>36</sup> and smaller cryptands.<sup>37</sup> The value for 15-crown-5 is approximately 0.015.

**X-ray Crystallography and FAB-MS Measurements.** The readiness with which **3** forms complexes with the smaller alkali metal ions was made apparent during our investigation of its synthesis. If the utmost care was not exercised to preclude the adventitious introduction of  $Li^+$  or  $Na^+$  ions, complexes would be isolated. The independent, purposeful preparation of the 2:1 sandwich complexes **27** and **28** provided crystals amenable to the acquisition of X-ray crystal structure data (Figures 2 and 3). Note that while **27** was obtained as a solvate with  $CH_2Cl_2$ , **28** was not. The counterion selected for this phase of the investigation was  $BF_4^-$  since this species does not coordinate to cations and thus favors sandwich formation.<sup>38</sup> As expected, the ligand configuration is the same in both complexes. The major difference resides in

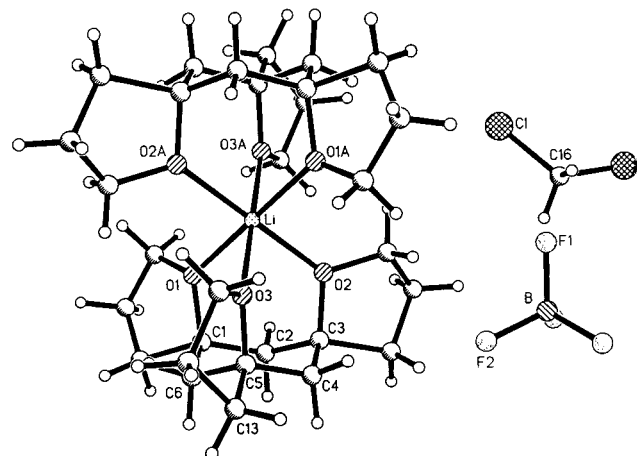


**Figure 2.** Perspective plot of the 2:1 sandwich complex of **3** with  $LiBF_4$  as the  $CH_2Cl_2$  solvate.

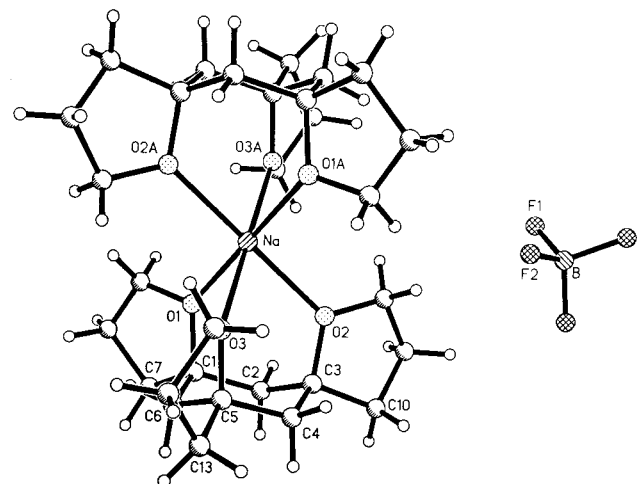
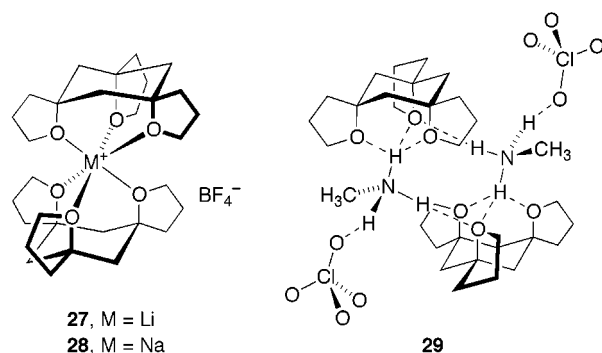


**Figure 3.** Perspective plot of the 2:1 sandwich complex of **3** with  $NaBF_4$ .

the distance at which the metal ion resides above the 01, 02, 03 plane. For  $Li^+$ , this value is 1.279 Å. The larger  $Na^+$  is somewhat further away at 1.553 Å.

The relative ratio of  $[(crown)_2 \cdot M]^+ / [(crown) \cdot M]^+$  peaks in FAB-MS has been used to correlate binding energies in sandwich complexes.<sup>39</sup> The intensity ratios for **27** and **28** were 0.1349 and 0.1571, respectively.



Cocrystallization of **3** and methylamine perchlorate from  $CH_2Cl_2$  gave clear crystals of a 1:1 hydrogen bonded complex **29** exhibiting a melting point of 94–96 °C (Figure 4). The hydrogen bond associates the complex into a dimer around a center of inversion. Each ammonium component forms six hydrogen bonds, with

(36) Cram, D. J.; Lein, G. M. *J. Am. Chem. Soc.* **1985**, *107*, 3657.  
 (37) Lehn, J.-M.; Sauvage, J. P. *J. Am. Chem. Soc.* **1975**, *97*, 6700.  
 (38) Hilgenfeld, R.; Saenger, W. *Top. Curr. Chem.* **1982**, *101*, 1.  
 (39) Takahashi, T.; Uchiyama, A.; Yamada, K. *Tetrahedron Lett.* **1992**, *33*, 3825.

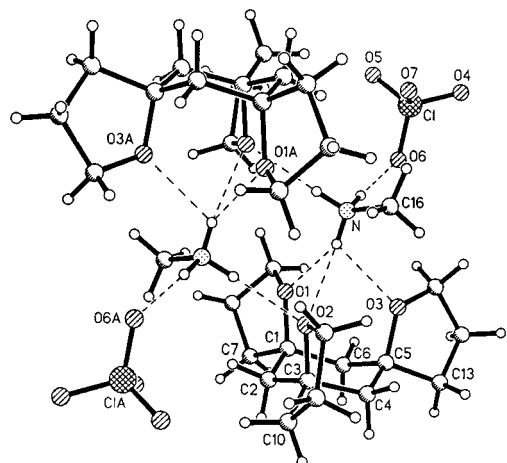


**Figure 4.** Perspective plot of the 2:1 complex of **3** with  $\text{CH}_3\text{NH}_3^+\text{ClO}_4^-$ .

H1–N involved with a single hydrogen bond to the anion and H3–N with a single hydrogen bond to O2 of one molecule of **3**. Interestingly, H2–N is directed toward the center of a second molecule of **3**, thus forming a trifurcated hydrogen bond with O1, O2, and O3.

**$^{13}\text{C}$  NMR Titration Experiments.** The conformational changes undergone by free ligands as they enter into metal complexation is often accompanied by significant changes in  $^{13}\text{C}$  NMR chemical shifts.<sup>40</sup> The complexing ability of **3** toward  $\text{LiClO}_4$  was probed by incremental titration in 4:1  $\text{CH}_3\text{CN}/\text{C}_6\text{D}_6$  at the normal operating temperature according to the reference procedure.<sup>41</sup> Upon the addition of 0.25 equiv of the lithium salt, a separate set of carbon signals attributable to the 2:1 complex appears (Figure 5). The next experimental point (total of 0.50 equiv) generates a spectrum which is exclusively that of the 2:1 sandwich. When this amount of salt is exceeded, the clearly defined signals of the 1:1 complex replace those seen earlier.

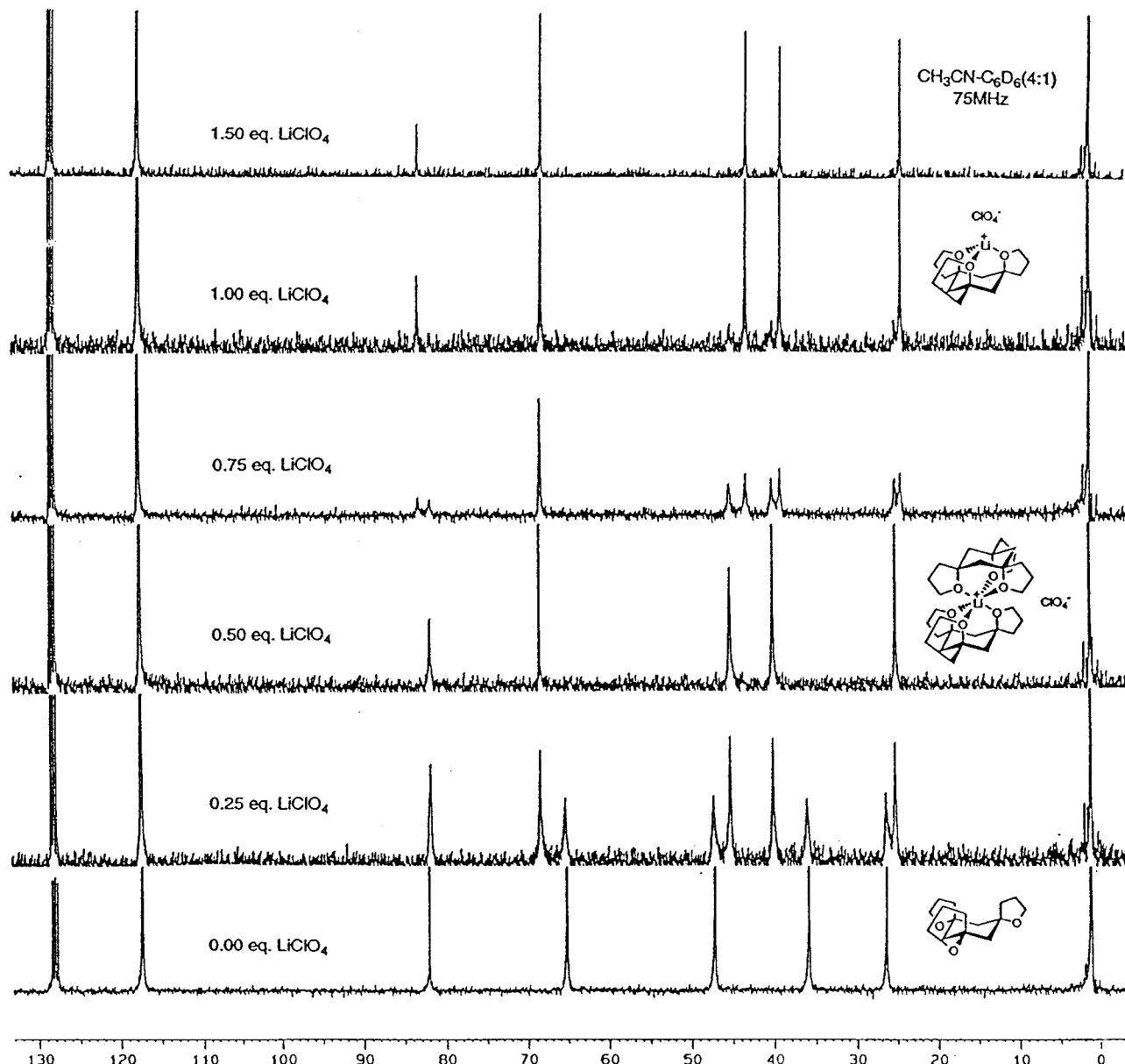


**Figure 5.** Incremental titration of **3** with  $\text{LiClO}_4$  in 4:1  $\text{CH}_3\text{CN}/\text{C}_6\text{D}_6$  with monitoring of the level of complexation by  $^{13}\text{C}$  NMR spectroscopy. The sequence of events is depicted from bottom to top.

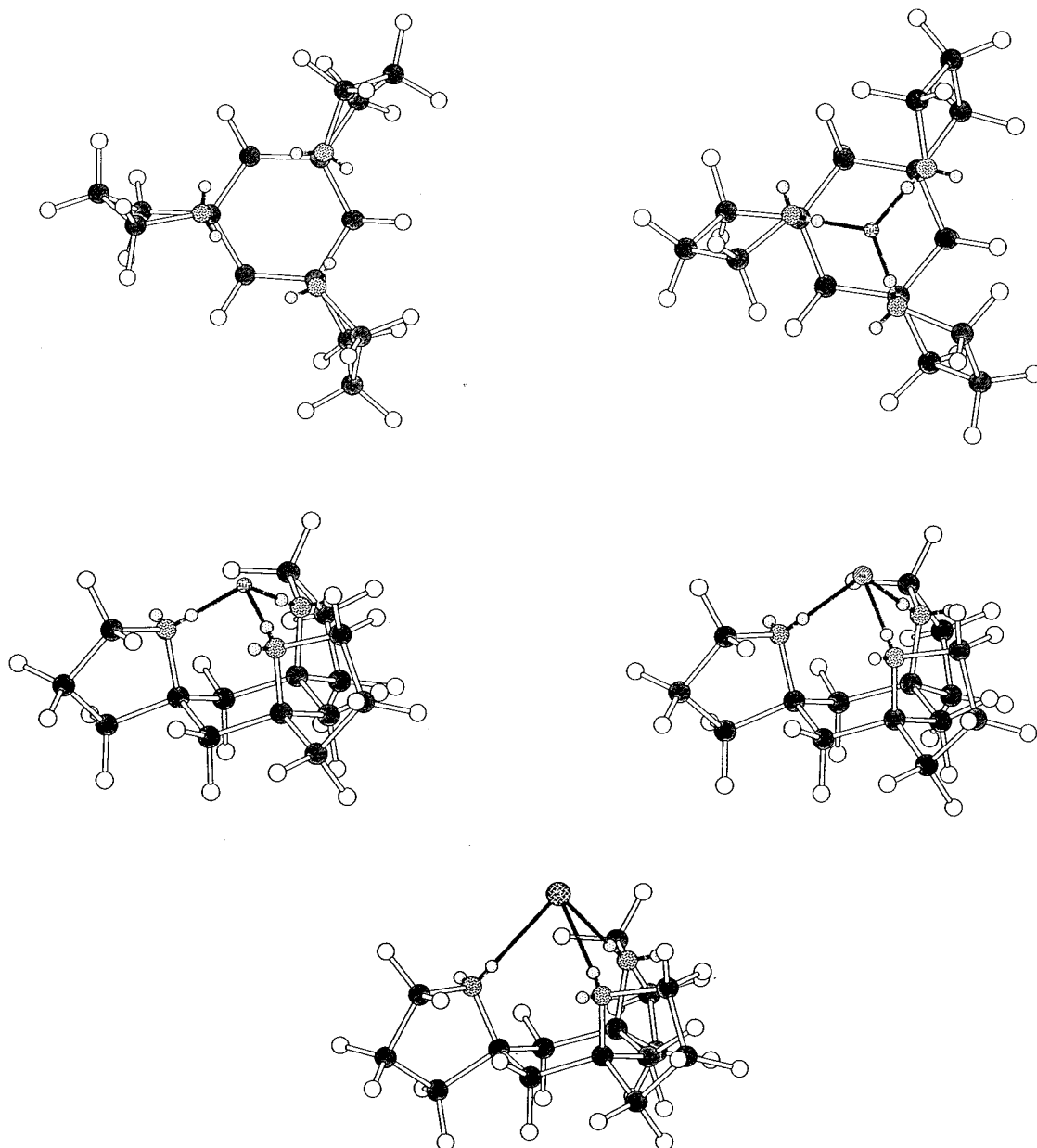


**Figure 6.** Top views of **3** as the free ligand and its complex to  $\text{Li}^+$  showing the differing arrangement of the nonbonded electrons on oxygen (top). Side views of the  $\text{Li}^+$ ,  $\text{Na}^+$  and  $\text{K}^+$  complexes to **3** showing the extent to which the metal ion protrudes above the ring (middle and bottom).

The appearance of separate sets of carbon signals is a direct consequence of slow exchange between the free ligand and its 2:1 complex, as well as between the 2:1 sandwich and the 1:1 complex (Scheme 6). The strong complexing stabilities witnessed earlier in the mass spectral measurements are equally well reflected in Figure 6. The changes in chemical shift suggest that a conformational change may be occurring upon metal complexation. Since the three ether oxygens must be axially disposed to allow **3** to serve as a ligand, the solution conformation of free **3** is likely the all-equatorial

arrangement as it is in the solid state. This partiality for equatorial oxygen occupancy is not seen in the simple monospiro example where **32a** is favored over **32e** by 2.1:1.<sup>43</sup>

The complexing capability of **3** toward  $\text{NaClO}_4$  is phenomenologically different. As seen in Figure 7, considerable line broadening sets in following the addition of 0.25 equiv of sodium ion. When a second identical increment of  $\text{NaClO}_4$  is introduced, sharp lines attributable to the 2:1 complex make their appearance. This spectrum does not change as more sodium perchlorate is added (up to 1.5 equiv). Thus, the 2:1 complex of **3** to  $\text{Na}^+$  is stable and not prone to conversion into the 1:1 complex under ordinary conditions, as in the case with lithium ion.

(40) For a recent example, consult: Hoffmann, R. W.; Münster, I. *Liebigs Ann./Recueil* **1997**, 1143.

(41) Fredriksen, S. B.; Dale, J. *Acta Chem. Scand.* **1992**, *46*, 1188.

(42) (a) Hay, B. P.; Rustad, J. R.; Hostetler, C. J. *J. Am. Chem. Soc.* **1993**, *115*, 11158. (b) Hay, B. P.; Rustad, J. R. *J. Am. Chem. Soc.* **1994**, *116*, 6316 and the many relevant references therein.

(43) Pederson, C. J.; Frensdorff, H. K. *Angew. Chem., Int. Ed. Engl.* **1972**, *11*, 16.

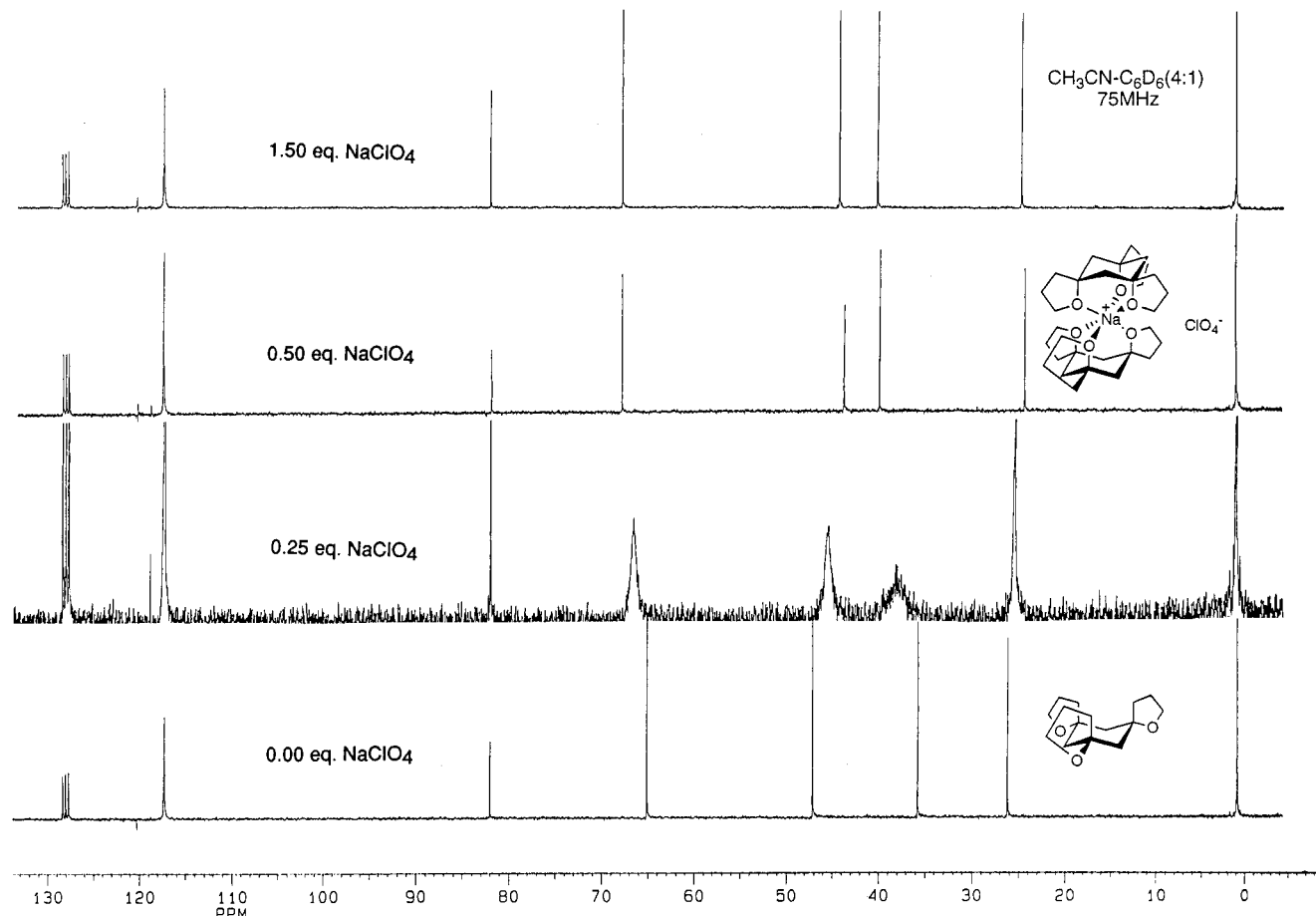
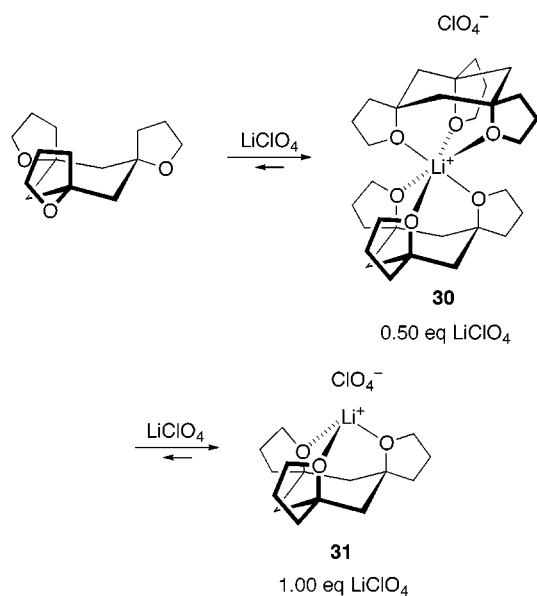
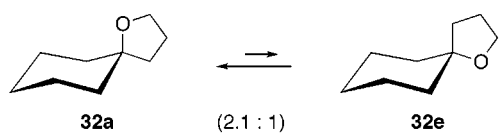


**Figure 7.** Incremental titration of **3** with  $\text{NaClO}_4$  in 4:1  $\text{CH}_3\text{CN-C}_6\text{D}_6$  with monitoring of the level of complexation by  $^{13}\text{C}$  NMR spectroscopy. Compare with Figure 5.

**Scheme 6**



**The Decomplexation Process.** Attempts to decomplex **31** by selective crystallization of **31** from 4:1 methanol/



water were unsuccessful. Alternatively, advantage was taken of the fact that **3** is freely soluble in ether and less soluble in water. Heating a suspension of **31** in 1:1 ether/water at the reflux temperature with vigorous stirring afforded 64% of **3** in the organic phase and 25% of recovered complex.

**Molecular Mechanics Study of the Alkali Metal Ion Complexes of **3**.** Several groups have found it informative to develop molecular mechanics models for the purpose of predicting the structures of ligands and their metal ion complexes as a means of evaluating the magnitude of steric strain within them. Most often, this has been done for a series of ligands that differ in structure but contain the same number and type of donor atoms.<sup>42</sup> For the present purposes, the *cis,cis* isomer **3** was first minimized in MODEL KS 2.96, thus obtaining its MM2-based energy (47.54 kcal/mol) and locating the nonbonding electron pairs residing at the three oxygen atoms (Figure 6). Thereby revealed was the preference of the free ligand to orient these filled orbitals approximately coplanar with the C–C bonds of the cyclohexene core.

For the computations involving the 1:1 lithium, sodium, and potassium complexes, the Macintosh-based CHEM-3D PLUS version 3.0 software package was found to properly orient the lone pairs toward the metal ion with attendant conformational modification of spirotetrahydrofuran conformation in all three pendant rings (Figure 6). We have adopted the working assumption that the force-field parameters used for arriving at the low-

**Table 2. Strain Energies and O–M Distances for **3** and Its Complexes by Means of MODEL KS 2.96 and CHEM-3D Parameters**

cation	CHEM-3D energy (kcal/mol)	MODEL energy (kcal/mol)	O–M distance (Å)
free ligand	47.54	47.54	
“distorted” ligand <sup>a</sup>			
Li <sup>+</sup>	69.89	70.05	1.839
Na <sup>+</sup>	73.28	73.45	2.145
K <sup>+</sup>	84.70	84.88	2.636

<sup>a</sup> The reported strain energies are for the conformations adopted in the respective complex after removal of the metal ion.

energy conformations of the complexes (see illustrations) were ideally suited to removal of the metal cations without disruption of the spatial orientation of the ligand. These “distorted ligands” were then examined for their CHEM-3D and MODEL MM2 energies without further processing. The results are compiled in Table 2.

As a consequence of the crystallographic data subsequently obtained for **27** and **28**, it is apparent that the atomic coordinates derived computationally for the O–M bond lengths overestimate the actual distances involved by 0.5–0.6 Å. Notwithstanding, the conformational realignment experienced by the trio of tetrahydrofuran rings, as required for proper bonding of the three oxygen centers to the metal ion, is clearly revealed. As the size of the central metal ion increases, **3** experiences progressive distortion of its carbocyclic framework in an attempt to accommodate proper 3-fold attachment to the metal. For the Li<sup>+</sup> → Na<sup>+</sup> progression, the energy difference is 3.4 kcal/mol. In our view, the necessity for this structural distortion is the major contributor to the ion selectivity of this ligand,  $K_a(\text{Li}^+)/K_a(\text{Na}^+) = 32$ . The even less preferred M–O bond length for the potassium complex, which involves an added energy increment in excess of 11 kcal/mol, reflects the size mismatch involved and the very substantive selectivity for lithium as  $K_a(\text{Li}^+)/K_a(\text{K}^+) = 2400$ . Consequently, in the present situation the size-match selectivity theory,<sup>43</sup> which states that a metal ion will form the most stable complex with a ligand that offers the best cavity size, and is frequently not adhered to by conformationally flexible systems,<sup>44</sup> may have validity because of prevailing structural rigidity arising from the spiroannulated rings.

### Summary

A stereocontrolled synthesis of the belted all-cis tripirotetrahydrofuran **3** has been accomplished in 17 steps from 3,5-dimethoxybenzoic acid in 14.6% overall yield. Whereas its cis,trans isomer **4** does not enter into complexation with alkali metal ions, **3** exhibits increased Li<sup>+/Na<sup>+</sup></sup> selectivity relative to 15-crown-5. The conversion of **3** into 2:1 sandwich complexes is general and leads to shelf-stable products. Tridentate ionophore **3** populates the **3eq** conformation in the solid state and in solution. For complexation to materialize, that conformation in which the three oxygen atoms converge on a small volume of space as in **3ax** must be adopted. The present data suggest that the **3eq** ⇌ **3ax** equilibrium is defined by a barrier high enough to show a single conformation on the NMR time scale, but of sufficiently low energy to allow for facile complexation. The backbone of **3** provides

considerable flexibility while defining a specific placement of the three heteroatoms which is particularly conducive to the binding of Li<sup>+</sup> and Na<sup>+</sup>. The design, synthesis, and complexation of new belted systems anticipated to have application as bifacial chelators, ion channel mimics, specific ion transport agents, and the like are underway.

### Experimental Section

**(5*R*,7*S*)-13-Methylene-1,8-dioxadispiro[4.1.4.3]tetradecane (16).** A mixture of **12** (900 mg, 2.69 mmol) and 10% palladium on charcoal (200 mg) in ethanol (30 mL) was stirred under an atmosphere of hydrogen (40 psi) for 3 h, filtered through a pad of Celite, and freed of solvent under reduced pressure to deliver 580 mg (95%) of the primary alcohol as a colorless liquid.

To a solution of this alcohol (510 mg, 2.25 mmol) and *o*-nitrophenylseleno-cyanate (615 mg, 2.70 mmol) in THF (10 mL) was added tri-*n*-butylphosphine (0.67 mL, 2.70 mmol). After 40 min of stirring, the solvent was removed and the residue was chromatographed on silica gel (elution with 50% ethyl acetate in hexanes) to afford the selenide, which was dissolved in THF (15 mL), cooled to –20 °C, and treated with 30% hydrogen peroxide (3.0 mL). The reaction mixture was maintained at –20 °C for 30 min, stirred at 20 °C for 16 h, poured into saturated NaHCO<sub>3</sub> solution (50 mL), and extracted with ether (20 mL) and CH<sub>2</sub>Cl<sub>2</sub> (2 × 20 mL). The combined organic phases were dried and concentrated in advance of chromatographic purification (silica gel, elution with 50% ethyl acetate in hexanes). There was isolated 368 mg (79% overall) of **16** as a colorless oil: IR (film, cm<sup>−1</sup>) 1651, 1449, 1337, 1072; <sup>1</sup>H NMR (300 MHz, C<sub>6</sub>D<sub>6</sub>) δ 4.62 (t, *J* = 1.4 Hz, 2 H), 3.73–3.58 (m, 4 H), 2.39 (d, *J* = 12.9 Hz, 1 H), 2.23–2.08 (m, 4 H), 1.78 (dt, *J* = 12.9, 1.9 Hz, 1 H), 1.70–1.50 (m, 6 H), 1.35–1.25 (m, 2 H); <sup>13</sup>C NMR (75 MHz, C<sub>6</sub>D<sub>6</sub>) ppm 145.0, 111.3, 82.7, 66.3, 49.2, 46.6, 34.8, 26.3; HRMS *m/z* (M<sup>+</sup>) calcd 208.1463, obsd 208.1460.

**(5α,7α,13β)-1,8,14-Trioxatrispiro[4.1.4.1.4.1]octadecane (4).** A solution of **16** (119 mg, 0.57 mmol) in 1:1 methanol/CH<sub>2</sub>Cl<sub>2</sub> (40 mL) was ozonolyzed at –78 °C and treated with methyl sulfide (3.0 mL). After overnight stirring, the solvent was evaporated and the residue was chromatographed on silica gel (elution with 25% ethyl acetate in hexanes) to afford the ketone, which was immediately dissolved in THF (5 mL), cooled to 0 °C, and treated with allylmagnesium bromide (2.4 mL of 1 N, 2.4 mmol). After 2 h at room temperature, the reaction mixture was quenched with saturated NH<sub>4</sub>Cl solution (10 mL), the separated aqueous layer was extracted with CH<sub>2</sub>Cl<sub>2</sub> (2 × 10 mL), and the combined organic phases were dried and concentrated. The residue was chromatographed on silica gel (elution with 25% ethyl acetate in hexanes) to afford the alcohol as a colorless oil.

To a cold (0 °C) solution of this alcohol in THF (5 mL) was added borane·THF complex (2.2 mL of 1 N in THF, 2.2 mmol). After being stirred for 1 h at this temperature, 3 N NaOH (2.2 mL) and 30% hydrogen peroxide were added. The reaction mixture was allowed to warm to 20 °C for 2 h, quenched with brine (10 mL) and CH<sub>2</sub>Cl<sub>2</sub> (10 mL), and processed in the prescribed manner to deliver the diol. The latter was dissolved in CH<sub>2</sub>Cl<sub>2</sub> (5 mL) and treated with tosyl chloride (185 mg, 0.97 mmol), triethylamine (0.20 mL, 1.43 mmol) and DMAP (10 mg). After 1 day, the reaction mixture was washed with water, dried, and concentrated. Chromatography of the residue (silica gel, elution with 25% ethyl acetate in hexanes) delivered 63 mg (44% overall) of **4** as a colorless liquid: IR (film, cm<sup>−1</sup>) 1448, 1349, 1177, 1047; <sup>1</sup>H NMR (300 MHz, C<sub>6</sub>D<sub>6</sub>) δ 3.75–3.60 (m, 4 H), 3.60–3.48 (m, 2 H), 2.15–1.95 (m, 3H), 1.75–1.40 (series of m, 15 H); <sup>13</sup>C NMR (75 MHz, C<sub>6</sub>D<sub>6</sub>) ppm 82.9, 82.5, 66.7, 65.9, 48.0, 45.9, 38.9, 36.7, 26.4, 25.2; HRMS *m/z* (M<sup>+</sup>) calcd 252.1725, obsd 252.1730.

Anal. Calcd for C<sub>15</sub>H<sub>24</sub>O<sub>3</sub>: C, 71.39; H, 9.59. Found: C, 71.10; H, 9.38.

**(5 $\alpha$ ,7 $\alpha$ ,13 $\alpha$ )-1,8,14-Trioxatrispiro[4.1.4.1.4.1]octadecane (3).** To a cold (0 °C) solution of **25** (272 mg, 1.08 mmol) in THF (10 mL) was added borane·THF complex (2.2 mL of 1 N in THF, 2.2 mmol). After 1 h at 0 °C, 3 N NaOH (2.2 mL) and 30% hydrogen peroxide (2.2 mL) were introduced, and the reaction mixture was warmed to room temperature for 2 h and quenched with brine (2 mL) and THF (20 mL). The separated aqueous layer was extracted with CH<sub>2</sub>Cl<sub>2</sub> (2 × 20 mL), and the predescribed workup followed. Chromatography on silica gel (elution with 50% ethyl acetate in hexanes containing 10% methanol) afforded the diol (242 mg, 83%) as a colorless liquid.

The above material was dissolved in CH<sub>2</sub>Cl<sub>2</sub> (20 mL) and treated with tosyl chloride (366 mg, 1.92 mmol), triethylamine (0.53 mL, 3.84 mmol), and DMAP (20 mg) at 20 °C for 6 h and at the reflux temperature for 15 h. After concentration, the residue was chromatographed on silica gel (elution with 50% ethyl acetate in hexanes) to afford 184 mg (81%) of **3** as colorless crystals, mp 111–113 °C (from 1:1 ether/hexanes), and 30 mg (11%) of the **(3)<sub>2</sub>·NaBF<sub>4</sub>** complex.

For **3**: IR (film, cm<sup>−1</sup>) 1454, 1222, 1044; <sup>1</sup>H NMR (300 MHz, CDCl<sub>3</sub>) δ 3.80 (t, *J* = 6.9 Hz, 6 H), 1.95–1.80 (m, 9 H), 1.70–1.65 (m, 6 H), 1.57 (d, *J* = 13.6 Hz, 3 H); <sup>13</sup>C NMR (75 MHz, CDCl<sub>3</sub>) ppm 81.5, 66.0, 45.5, 37.5, 25.3; HRMS *m/z* (M<sup>+</sup>) calcd 252.1725, obsd 252.1712.

Anal. Calcd for C<sub>15</sub>H<sub>24</sub>O<sub>3</sub>: C, 71.39; H, 9.59. Found: C, 71.28; H, 9.56.

**Formation of the Lithium Tetrafluoroborate Complex 27.** A 24 mg (0.095 mmol) sample of **3** was added to a solution of lithium tetrafluoroborate (4.5 mg, 0.048 mmol) in CH<sub>3</sub>CN (2 mL), stirred overnight, and freed of solvent. Recrystallization of the residue from 20% CH<sub>2</sub>Cl<sub>2</sub> in hexanes) afforded 20 mg (70%) of **27** as colorless crystals, mp >290 °C dec; <sup>1</sup>H NMR (300 MHz, CDCl<sub>3</sub>) δ 3.76 (t, *J* = 6.2 Hz, 6 H), 1.95–1.70 (m, 15 H), 1.55 (d, *J* = 14.0 Hz, 3 H); <sup>13</sup>C NMR (75 MHz, CDCl<sub>3</sub>) ppm 81.6, 68.1, 45.3, 39.7, 25.0; positive FAB MS *m/z* for **3·Li<sup>+</sup>** calcd 259, obsd 259.15 (100%); for **(3)<sub>2</sub>Li<sup>+</sup>** calcd 511, obsd 511.42 (13.5%).

Anal. Calcd for C<sub>30</sub>H<sub>48</sub>BF<sub>4</sub>LiO<sub>6</sub>: C, 60.21; H, 8.08. Found: C, 60.14; H, 7.95.

**Formation of the Sodium Tetrafluoroborate Complex 28.** A solution of **3** (38 mg, 0.15 mmol) in 1:1 aqueous acetonitrile (4 mL) containing sodium tetrafluoroborate (8.3 mg, 0.75 mmol) was stirred overnight, freed of solvent to leave a residue that was crystallized from 20% CH<sub>2</sub>Cl<sub>2</sub> in hexanes to furnish 30 mg (65%) of **28** as colorless crystals: mp >295 °C dec; <sup>1</sup>H NMR (300 MHz, CDCl<sub>3</sub>) δ 3.78 (t, *J* = 6.6 Hz, 6 H),

1.91–1.80 (m, 9 H), 1.75–1.70 (m, 6 H), 1.52 (d, *J* = 14.0 Hz, 3 H); <sup>13</sup>C NMR (75 MHz, CDCl<sub>3</sub>) ppm 81.8, 67.7, 44.5, 40.0, 24.6; positive FAB MS *m/z* for **3·Na<sup>+</sup>** calcd 275, obsd 275.16 (100%); for **(3)<sub>2</sub>Na<sup>+</sup>** calcd 527, obsd 527.22 (15.7%).

Anal. Calcd for C<sub>30</sub>H<sub>48</sub>BF<sub>4</sub>NaO<sub>6</sub>: C, 58.64; H, 7.87. Found: C, 58.82; H, 7.76.

**Formation of the Methylammonium Perchlorate Complex 29.** A solution containing 50 mg (0.20 mmol) of **3** and 130 mg (0.99 mmol) of methylammonium perchlorate in CH<sub>3</sub>CN (3 mL) was stirred overnight at room temperature. After solvent evaporation, CH<sub>2</sub>Cl<sub>2</sub> (3 mL) was introduced and the unreacted amine salt was filtered off. The filtrate was concentrated and the residue was triturated with dry ether. After decantation, 20 mg of **3** was recovered. Recrystallization of the remaining solid from CH<sub>2</sub>Cl<sub>2</sub> afforded 40 mg (50%) of **29** as colorless crystals: mp 94–96 °C; <sup>1</sup>H NMR (300 MHz, CDCl<sub>3</sub>) δ 3.83 (t, *J* = 6.9 Hz, 6 H), 2.65 (q, *J* = 6.2 Hz, 3 H), 1.95–1.80 (m, 9 H), 1.75–1.60 (m, 6 H), 1.49 (d, *J* = 14.0 Hz, 3 H); <sup>13</sup>C NMR (75 MHz, CDCl<sub>3</sub>) ppm 81.5, 66.7, 44.7, 38.8, 25.6, 24.8; positive FAB MS *m/z* for **3·H<sup>+</sup>** calcd 253, obsd 253.21 (100%); for **3·CH<sub>3</sub>NH<sub>3</sub><sup>+</sup>** calcd 284, obsd 284.21 (69.7%).

**<sup>13</sup>C NMR Titration Studies.** A solution of **3** (50 mg, 0.20 mmol) in 4:1 CH<sub>3</sub>CN/C<sub>6</sub>D<sub>6</sub> was placed in an NMR tube. A separate solution of LiClO<sub>4</sub> (32 mg, 0.30 mmol) in the same solvent system (1.2 mL) was prepared. A <sup>13</sup>C NMR spectrum was recorded after incremental addition of 0.20 mL (0.25 equiv) aliquots of the perchlorate salt up to 1.5 equiv of LiClO<sub>4</sub>.

The resulting NMR solution was evaporated and the CH<sub>2</sub>Cl<sub>2</sub>-soluble complex was recrystallized from CH<sub>2</sub>Cl<sub>2</sub> to furnish 65 mg (92%) of **31** as colorless crystals, mp 254–256 °C. The latter were used for decomplexation studies described above.

**Acknowledgment.** We thank the National Science Foundation and Hoechst Marion Roussel for partial financial support of this research and Dr. Kurt Loening for assistance with nomenclature.

**Supporting Information Available:** Experimental procedures and spectroscopic data for all compounds not described in the printed format, details of the complexation studies, and X-ray structure reports for **3**, **[3]<sub>2</sub>·LiBF<sub>4</sub>·CH<sub>2</sub>Cl<sub>2</sub>**, **[3]<sub>2</sub>·NaBF<sub>4</sub>**, and **29**. This material is available free of charge via the Internet at <http://pubs.acs.org>.

JO001430A